

1

2

3

4

5

6

7

8

9

10

11

12

13

14

15

16

17

18 *Harvard University, Cambridge, MA, USA*

19 Charles G. Bardeen

20 *National Center for Atmospheric Research, Boulder, CO, USA*

21 Owen B. Toon and Bruce C. Kindel

22 *University of Colorado, Boulder, CO, USA*

23 Paul A. Newman and Matthew J. McGill

24 *NASA Goddard Space Flight Center, Greenbelt, MD, USA*

25 Dennis L. Hlavka

26 *Science Systems and Applications, Inc., Greenbelt, MD, USA*

27 Leslie R. Lait

28 *Morgan State University, Baltimore, MD, USA*

29 Mark R. Schoeberl

30 *Science and Technology Corporation, Columbia, MD, USA*

31 John W. Bergman

32 *Bay Area Environmental Research Institute, Sonoma, CA, USA*

33 Henry B. Selkirk

34 *University Space Research Association, Greenbelt, MD, USA*

35 M. Joan Alexander and Ji-Eun Kim

36 *NorthWest Research Associates, CoRA Office, Boulder, CO, USA*

37

Boon H. Lim

38

Jet Propulsion Laboratory, Pasadena, CA, USA

39

Jochen Stutz

40

University of California, Los Angeles, CA, USA

41

Klaus Pfeilsticker

42

University of Heidelberg, Heidelberg, Germany

43 *Corresponding author address: NASA Ames Research Center, MS 245-5, Moffett Field, CA

44 94035.

45 E-mail: eric.j.jensen@nasa.gov

ABSTRACT

46 The February through March 2014 deployment of the NASA Airborne Trop-
47 ical TRopopause EXperiment (ATTREX) provided unique in situ measure-
48 ments in the western Pacific Tropical Tropopause Layer (TTL). Six flights
49 were conducted from Guam with the long-range, high-altitude, unmanned
50 Global Hawk aircraft. The ATTREX Global Hawk payload provided mea-
51 surements of water vapor, meteorological conditions, cloud properties, tracer
52 and chemical radical concentrations, and radiative fluxes. The campaign was
53 partially coincident with the CONTRAST and CAST airborne campaigns
54 based in Guam using lower-altitude aircraft (see companion articles in this
55 issue). The ATTREX dataset is being used for investigations of TTL cloud,
56 transport, dynamical, and chemical processes as well as for evaluation and im-
57 provement of global-model representations of TTL processes. The ATTREX
58 data is openly available at <https://espoarchive.nasa.gov/>.

1. Introduction

The NASA Airborne Tropical Tropopause EXperiment (ATTREX) was a five-year airborne science program focused on the physical processes occurring in the Tropical Tropopause Layer (TTL, $\approx 13\text{--}19$ km). Inasmuch as the Brewer-Dobson circulation transports air upward through the TTL and then throughout the entire stratosphere, processes controlling TTL composition provide a boundary condition for stratospheric composition. A particular focus of ATTREX is the dehydration of air entering the stratosphere by ice crystal growth and sedimentation near the cold tropical tropopause. Radiative transfer calculations show that even small changes in stratospheric humidity have climate impacts that are significant compared to those of decadal increases in greenhouse gases (??). While the tropospheric water vapor-climate feedback is well represented in global models, predictions of future changes in stratospheric humidity are highly uncertain because of gaps in our understanding of physical processes occurring in the TTL. Uncertainties in the TTL transport processes and chemical composition also limit our ability to predict future changes in stratospheric ozone. The 2014 ATTREX deployment to Guam was particularly valuable for addressing these science issues given that the lowest tropopause temperatures, driest TTL air, and strongest upward transport occur in the western Pacific during Boreal wintertime.

Stratospheric humidity and chemical composition are controlled by a complex interplay of processes occurring in the TTL (Figure 1). Deep convection links surface conditions to the upper troposphere. The strength and depth of convection impacts transport of water vapor and chemical constituents to the TTL and deep convection is the predominant source of tropical waves. Tropical waves affect TTL thermal structure cirrus formation and wave breaking and dissipation in the stratosphere drive large scale ascent in the tropics. Ubiquitous TTL cirrus have a direct effect on the Earth's radiation budget, and their regulation of stratospheric humidity results in an indi-

rect radiative effect. TTL processes also influence the stratospheric ozone layer. Since precursors of ozone-depleting substances pass through the TTL before reaching the stratosphere, the TTL composition has a controlling influence on rates of stratospheric ozone destruction (?).

The ATTREX campaigns used the long-range (16,000 km), high-altitude (20 km) NASA Global Hawk unmanned aircraft system for TTL measurements (Figure 2). The ATTREX Global Hawk payload consisted of twelve instruments measuring cloud properties, water vapor, meteorological conditions, chemical tracers, chemical radicals, and radiation (see Table 1). The overall ATTREX project was managed by the NASA Ames Research Center, and the Global Hawk program is managed by Armstrong Flight Research Center (AFRC, formerly Dryden Flight Research Center). Prior to the Guam deployment, two ATTREX flight series were conducted out of AFRC, providing measurements in the central and eastern Pacific TTL (see ? for details). We report here on the January–March, 2014 ATTREX deployment to Guam (13°28'0" N, 144°46'59" E), which provided measurements in the western Pacific.

2. ATTREX Global Hawk Payload

The ATTREX payload was designed to address key uncertainties in our understanding of TTL composition, transport, and cloud processes affecting water vapor and short-lived trace gases. Measurements of water vapor, cloud properties, numerous chemical tracers, key radical species, meteorological conditions, and radiative fluxes were included (Table 1). Instruments were chosen based on proven techniques and size/weight accommodation on the Global Hawk.

The very dry conditions present in the tropical tropopause region (H_2O mixing ratios as low as $\simeq 1$ ppmv) represent a significant challenge for accurately measuring water vapor. Large, unresolved discrepancies between past water vapor concentrations measured with different instruments

(??) have generally precluded use of the measurements for detailed studies of cloud microphysical processes.

The water vapor measurement challenges were addressed in ATTREX by including two complementary instruments, namely Diode Laser Hygrometer (DLH) and NOAA Water (NW), both of which have suitable sensitivity for measuring water vapor values as low as 1 ppmv. The NW instrument (added to the payload in 2013) provides a closed-cell tunable-diode laser (TDL) measurement that includes the in-flight calibration system used on the NOAA chemical ionization mass spectrometer (CIMS) instrument during MACPEX (?). Calibration during the flights avoids the uncertainty associated with assuming that ground-based calibrations apply to in-flight conditions. The NW instrument also measures total water concentration using a forward-facing inlet that enhances ice concentration. The DLH instrument provides an open-path TDL measurement by firing the laser from the fuselage to a reflector on the wing and measuring the return signal. The path length (12.2 m) is long enough to provide a precise, fast measurement of water vapor. The precision is sufficient to permit detection of fine structure in the TTL water vapor field even at a data rate approaching 100 Hz. With typical flights speeds of 170 m s^{-1} and ascent/descent rates of 10 m s^{-1} , DLH provides measurements with spatial resolution determined by the geometry of its optical path: about 6 m horizontally and less than 0.5 m vertically. Temperature, pressure, and wind measurements were made with the Meteorological Measurement System (MMS) that also provided high-frequency data (up to 20 Hz) and permits examinations of fine structures in the relative humidity field and their correlation with cloud variations (?).

We have a high level of confidence in the estimated accuracy of the DLH and NW measurements ($\simeq 5\text{--}10\%$) for two reasons: (1) The NW and DLH data obtained in the 2013 and 2014 flights show a high degree of consistency and agreement for TTL H_2O values less than 10 ppmv (see Figure 7). (2) In TTL cirrus with very high ice concentrations (in excess of 1 cm^{-3}) the relative humidity

with respect to ice (RH_{ice}) is consistently near 100% (?). The time scale for quenching of super-/sub-saturation by ice crystal growth/sublimation in such clouds is a few minutes or less such that the RH_{ice} is expected to remain near 100%.

For the Guam ATTREX flights, TTL cirrus microphysical properties were measured with the Spec Inc. Hawkeye instrument. Hawkeye is a combination of two imaging instruments (equivalent to the two-dimensional Stereo probe (2D-S) (?) and Cloud Particle Imager (CPI) (?)), and a spectrometer (equivalent to the Fast Cloud Droplet Probe (FCDP) (?)), all of which have been used in the past for airborne cloud measurements. For consistency and comparison with the 2011 and 2013 ATTREX flight series, a stand-alone FCDP was also included in the Guam payload. The combination of FCDP and 2D-S probes provides ice crystal size distributions spanning crystal maximum dimensions from about 1 μm to about 4 mm. The CPI provides detailed ice crystal images that can be used to determine habit information for crystals with maximum dimensions larger than about 40 μm . The cloud measurements, along with the water vapor and temperature measurements, are being used to test our theoretical understanding of ice crystal nucleation, depositional growth, and sedimentation (e.g. ???).

The ATTREX payload included a number of tracer measurements that can be used to quantify TTL transport pathways and time scales. The Harvard University Picarro Cavity Ringdown System (HUPCRS) provides precise, stable measurements of CO_2 and CH_4 . The HUPCRS also includes a CO channel that provides useful data with some averaging. The UAS Chromatograph for Atmospheric Trace Species (UCATS) provides measurements of O_3 , N_2O , SF_6 , H_2 , CO (tropospheric), and CH_4 , as well as an additional measurement of water vapor.

The Global Hawk Whole Air Sampler (GWAS) provides 90 gas canister samples per flight. The times for the GWAS samples were determined on a real-time basis depending on the flight plan. Post-flight, gas chromatographic analysis provides concentrations of a plethora of trace gases with

152 sources from industrial mid-latitude emissions, biomass burning, and the marine boundary layer,
153 with certain compounds (e.g. organic nitrates) that have a unique source in the equatorial surface
154 ocean. GWAS also measures a full suite of halocarbons that provide information on the role of
155 short-lived halocarbons on chemistry in the tropical UTLS region, on halogen budgets in the UTLS
156 region, and on trends of HCFCs, CFCs, and halogenated solvents.

157 The ATTREX payload also included radiation measurements, which will be used to quantify
158 the impacts of clouds and water vapor variability on TTL radiative fluxes and heating rates. The
159 spectral solar flux radiometer (SSFR) measurements additionally provide information about cir-
160 rus microphysical properties, and retrieval of TTL water vapor amounts with SSFR spectra has
161 been demonstrated (?). Lastly, the Differential Optical Absorption Spectrometer (mini-DOAS)
162 instrument provides measurements of BrO, NO₂, O₃, IO, O₄, H₂O, and cloud/aerosol extinction
163 at various elevation angles near the limb. These measurements can be converted to vertical trace
164 gas concentration profiles from 1 km above to 5 km below flight altitude using radiative transfer
165 calculations and either optimal estimation or O₃ absorption techniques. The combination of the
166 mini-DOAS BrO (and IO) measurements and GWAS measurements of major halogenated hydro-
167 carbons provides constraints on the TTL and lower stratospheric Br_y and I_y budgets.

168 Two additional remote-sensing instruments were included that provide both valuable sci-
169 ence data and real-time information for flight operations. The Cloud Physics Lidar (CPL) provides
170 profiles of aerosol/cloud backscatter and depolarization below the aircraft. The high sensitivity of
171 CPL backscatter measurements have proven useful for detecting tenuous TTL cirrus (?), and the
172 depolarization measurement provides information about ice crystal habits. The Microwave Tem-
173 perature Profiler (MTP) provides vertical profiles of temperature above and below the aircraft. The
174 CPL and MTP data was transmitted to the Global Hawk ground operations center via a high-speed

data link, and the information was used to determine when to execute vertical profiles through the TTL.

3. ATTREX 2014 Global Hawk Flights

The overall ATTREX project included multiple campaigns: flights were conducted out of AFRC in the fall of 2011 and the winter-spring of 2013 (see ? for details). Here, we report on the 2014 deployment to Guam in the western Pacific during February and early March, 2014. The flight paths for the six Guam Global Hawk flights are shown in Figure 3, along with the earlier ATTREX flights for context. The Coordinated Airborne Studies in the Tropics (CAST) and the CONvective TRansport of Active Species in the Tropics (CONTRAST) campaigns were planned to be concurrent with the ATTREX Guam flights. The CAST and CONTRAST campaigns are described in separate articles in this issue. A series of aircraft operations problems delayed the Global Hawk flights until the CAST and CONTRAST operations were essentially completed. Nevertheless, the combined lower- to middle-troposphere sampling from CAST and CONTRAST flights and upper troposphere/lower stratosphere ATTREX Global Hawk measurements provide unique information about the western tropical Pacific atmospheric composition from the surface to the stratosphere.

The Guam flights provided an extensive survey of western Pacific TTL composition. Details of the individual Global Hawk flights from Guam are provided in Table 2. The general sampling strategy was to execute numerous vertical profiles between 45,000 ft (\simeq 13.7 km) and cruise altitude (53,000–60,000 ft (\simeq 16.2–18.3 km), depending on the fuel load). Figure 4 shows the resulting coverage in longitude, latitude, and height space. Global Hawk power constraints forced us to turn off the GWAS pumps on descents; thus, GWAS samples were taken during the ascents only.

197 The transit from AFRC to Guam on 16–17 January, 2014 served primarily to transport the Global
198 Hawk to the deployment location. Concerns about fuel consumption and limited ability to transmit
199 commands to the aircraft payload during the flight precluded execution of vertical profiles through
200 the TTL. The aircraft cruised near the tropical tropopause for most of the flight. As mentioned
201 above, aircraft operational and mechanical problems (as well as unusually severe local weather
202 in Guam) prevented Global Hawk flights for the next several weeks after arrival in Guam while
203 CONTRAST and CAST were underway.

204 The prevailing meteorological pattern in the Boreal winter western Pacific TTL has a pool of
205 cold temperatures located just east of the most active convection (?) (see Figure 3). These cold
206 temperatures are essentially a wave response to the convective heating and uplift; as part of this
207 wave response, there is a Boreal hemisphere anticyclone, usually centered north and slightly east
208 of the cold temperature pool. There is frequently a corresponding anticyclone in the southern
209 hemisphere, though this was typically out of range of ATTREX sampling. The convection (which
210 is strongest in the southern hemisphere during Boreal winter, though there is significant penetration
211 to northern hemisphere latitudes – Figure 3) is modulated by the Madden-Julian Oscillation (MJO,
212 ?). This oscillation produces substantial fluctuations in the position and intensity of the cold
213 temperature pool and the associated anticyclone. The primary research flights occurred during the
214 period 12 February through 13 March, during which time the cold pool and anticyclone basically
215 moved from well west of Guam to the central Pacific, roughly consistent with the propagation
216 of the MJO. The progression of the center of the anticyclone with the various research flights is
217 shown by the “X” symbols in Figure 3.

218 The first ATTREX local flight from Guam (RF01) occurred on 12-13 February. The primary
219 focus of this flight was to survey the composition, humidity, clouds, and thermal structure of the
220 western Pacific TTL. During this flight, convection was most active well west of Guam and sup-

221 pressed at Guam's longitudes, so the center of monsoon anticyclone (Figure 3) and the coldest
222 TTL temperatures were also west of Guam. A semi-Lagrangian flight plan, approximately along
223 the streamlines of the anticyclone was chosen, arcing north and west of Guam, and then reversing
224 course and heading south of Guam down to near the equator. Limitations on Global Hawk opera-
225 tions in cold temperatures and aerodynamic drag prevented the aircraft from climbing above about
226 57,000 ft (17.8 km). Cirrus clouds were observed throughout the TTL, almost certainly formed in
227 situ because of the absence of nearby convection. Given the westward position of the anticyclone,
228 the TTL circulation was from the west northwest, and back trajectory analysis showed that a sig-
229 nificant portion of the air sampled had progressed clockwise around the anticyclone after having
230 been detrained from convective systems in Africa about a week to 10 days prior to the time of ob-
231 servation. The CO₂ and methane measurements were consistent with this picture. The trajectory
232 method used is similar to that described in ? and ?. That is, diabatic back trajectories are calcu-
233 lated from clusters of points surrounding the aircraft measurements using ERA-Interim analyses
234 and observed diabatic heating rates typical for the Boreal winter season (?). These back trajectories
235 are routed through 3-hourly fields of cloud top potential temperature derived from global infrared
236 brightness temperatures, global rainfall rates, and analysis temperatures. Convective influence is
237 said to occur if an air parcel is over a convective system, and its potential temperature is lower
238 than the cloud top potential temperature. The method allows calculation both of the time to most
239 recent convection for a given sampled air parcel, and the location of that most recent convection.
240 allowing air from African convection to be sampled, which was apparent in the CO₂ and methane
241 measurements.

242 The second flight (RF02 16–17 February) occurred as the monsoon anticyclone was reforming
243 east of Guam. There was very active convection about 7 degrees south of Guam, which undoubt-
244 edly contributed to the substantial change in the anticyclone's position. Shortly after takeoff on

245 RF02, the primary satellite communications system for Global Hawk command and control (IN-
246 MARSAT) was discovered to be inoperative. As a result, the aircraft was forced to stay within line
247 of sight of the ground station on Guam. The aircraft circled in the zone next to Guam reserved for
248 unmanned aircraft climbout and final descent for 17.5 hours providing 26 vertical profiles through
249 the TTL. This turned out to be an interesting location to profile on this day, with a distinct double
250 cold point temperature structure and corresponding vertical lamination in tracer concentrations
251 that is related to the wave motions (?). TTL cirrus streaming over Guam from deep convection to
252 the southeast was sampled much of the time on this flight. The stationary position of the aircraft
253 over Guam allowed high time resolution sampling of an inertia-gravity wave with a peak-to-peak
254 amplitude of about 5 K. This wave contributed to the in situ formation of observed TTL cirrus at
255 the cold point near 17.7 km altitude. The CAST and CONTRAST aircraft (NERC BAe-146 and
256 NSF G-5) sampled near the Global Hawk flight path on this day.

257 For the remainder of February, convection continued to strengthen just south of Guam, consistent
258 with the onset of the active phase of the Madden Julian Oscillation (MJO). In response, the upper
259 level anticyclone was pushed east of Guam, along with the coldest tropopause temperatures. As
260 preparations for RF03 were underway around the beginning of March, a tropical cyclone was
261 developing southeast of Guam. By the time of RF03 on 4–5 March, cyclone Faxai had swept
262 northward east of Guam and briefly reached typhoon status around the time the Global Hawk
263 sampled the TTL in the vicinity of the storm (see Figure 5). The flight path took the aircraft
264 northwest from Guam and then along an eastbound leg just south of the cyclone. Multiple vertical
265 profiles were executed through the outflow cirrus emanating from the cyclone. Except for a few
266 occasions at the highest altitudes, the observed flow was from the south and southwest, so the
267 air sampled during multiple vertical profiles was about 0.5–2 days old, having detrained from the
268 cyclone when it was actually south of the flight track. Temperatures were sufficiently cold (the

coldest measured temperatures during the ATTREX Guam flights) to maintain (or reform) the outflow cirrus from the cyclone over that period of time. The TTL cirrus tops were as high as 17.3 km. The flight provides an excellent case study of TTL composition perturbation by deep, organized convection.

The tropical cyclone sampled by RF03 marked the beginning of a shift of convection toward the southern hemisphere, a weakening of the monsoon anticyclone, and a clear eastward propagation of the MJO. In response to the shift in convection, the coldest temperatures moved into the southern hemisphere. The 6–7 March (RF04) flight took place in this environment, providing an additional survey of western Pacific TTL tracers and cirrus. The aircraft was directed south to 6°N and then flew a long, approximately constant-altitude leg at this latitude where multiple radiosonde stations are located, with the objective of characterizing wave properties with the combination of MMS and MTP measurements and the radiosondes. Because of the weakening anticyclone and shift of cold temperatures and convection to the southern hemisphere, this flight had temperatures about 3 K warmer than typical of the other flights. (The minimum temperature for RF04 was about 188 K.) The amount of fresh (less than 2 days) convective injection was notably less than during RF03, though there was significant convective influence about 3–5 days old from the strong MJO that had dominated the last two weeks of February. Even though temperatures were warmer in RF04 than in the other flights, some of the highest thin cirrus (up to 17.9 km) was observed on this flight.

The fifth local flight (RF05) on 9–10 March served as a southern survey and included considerable sampling in the outflow of strong convection. The goal was to reach about 20°S, but the aircraft had to turn back near 12°S due to a line of intense convection that developed at about 17°S reaching the cold point tropopause at about 17 km. Tropical cyclone Lusi was developing at 15°S just east of the flight track. Cirrus with high ice water content and numerous ice crystals

was sampled up to the cold-point tropopause along the southernmost leg of the flight. Prevailing winds at flight level were from the east and southeast, so this airmass originated from the line of convection to the south.

Flight RF06 on 11–12 March served as a northern survey and was confined to latitudes north of 10°N, with multiple vertical profiles on both the tropical and extra-tropical sides of the subtropical jet. Two of the profiles north of the jet extended down to 43,000 ft ($\simeq 13.1$ km) in order to sample as much of the extra-tropical lowermost stratosphere as possible. The objective of this flight was to provide tracer measurements both in the TTL and in the extratropical lower stratosphere for quantification of the role of in-mixing on TTL composition. As in the case for RF05, both convection and the coldest temperatures were south of the equator, so very little fresh convection was noted on this flight. A developing trough in the midlatitude western Pacific moved the boundary between midlatitude and tropical air southward, making the midlatitude air more accessible for sampling. Minimum temperatures were typically about 189 K in RF06, substantially warmer than the other flights. As had been the case since RF03, the anticyclone was east of Guam (Figure 3) resulting in northward and northwestward flow over the tropical portion of the track. Aged convective outflow from the South Pacific Convergent Zone was apparent in the tracers. Close to the end of the flight, the aircraft passed over a line of convection southeast of Guam, with cloud tops at about 15.5 km. Temperature fluctuations were observed during this passage, with the lowest temperatures of the flight observed (about 187.5 K). The aircraft was able to descend downstream of this convection and sample the outflow.

The transit back to AFRC provided the first opportunity to perform vertical profiling in the central Pacific (since the transit from AFRC to Guam was entirely at cruise altitude). At this time convection was reforming north of the equator, but consistent with the eastward propagation of the MJO, the convection was well east of Guam. In response to the increased northern hemisphere

317 convection, cold temperatures in the TTL moved north and occupied a large area centered on the
318 equator and east of the convection (and east of the dateline). For the most part, the gradual climb
319 to 17 km during the first 6 hours of the flight was in relatively warm temperatures and downstream
320 of a large, deep convective system with cloud tops up to the cold point tropopause. During this
321 portion of the flight, a layer of ice crystals and freshly lofted air (age about a day) was observed,
322 with minimum temperatures of $\simeq 192$ K. About 6 hours into the flight, as the aircraft crossed the
323 dateline, vertical profiling in the cold pool commenced. Temperatures were 5 K colder east of the
324 dateline, the air was considerably older (3 days to a week, depending on altitude, with the older
325 air at higher altitudes), and substantial cirrus were observed. The transit back to AFRC provided
326 an additional survey of TTL composition across the western and central Pacific.

327 **4. Overview of ATTREX measurements**

328 It was recognized in the ATTREX planning stage that the Boreal wintertime western Pacific is
329 a region with very high occurrence frequency of clouds in the TTL (?), and the ATTREX Guam
330 flights provided a wealth of TTL cirrus measurements. As indicated by the Hawkeye measure-
331 ments, the Global Hawk was inside TTL cirrus more than 34 hours during the flights from Guam.
332 Figure 6 shows examples of ice crystal images and size distributions provided by Hawkeye. The
333 CPI images often indicated bullet rosette habits and lack of evidence for ice crystal aggregates
334 even on flight segments in cirrus that appeared to be associated with deep convection. The exis-
335 tence of bullet rosettes is generally an indication of in situ nucleation and growth of ice crystals,
336 whereas aggregates are typically observed in fresh anvil cirrus (?). The ATTREX data supports
337 earlier results indicating that in situ nucleation and/or deposition growth of anvil ice crystals are
338 important processes for generating and maintaining extensive cirrus shields around tropical deep
339 convection (?).

340 As discussed above, the ATTREX DLH and NOAA-WV instruments provided accurate, precise
 341 water vapor measurements. Figure 7 shows frequency distributions of TTL relative humidity with
 342 respect to ice from the Guam flights as well as a comparison between DLH and NWV. The strong
 343 peak near $RH_{ice}=100\%$ is expected since vapor deposition on and sublimation from cirrus ice
 344 crystals will tend to drive the water vapor concentration toward ice saturation. Consistent with ice
 345 nucleation and growth theory, substantial supersaturations with respect to ice occur frequently in
 346 the TTL (?). The observations of large ice supersaturations indicates that the dehydration of air
 347 passing through the TTL is less efficient than currently assumed in global models, and the model
 348 representations of TTL cirrus processes need to be modified to include supersaturation both in
 349 clear-sky regions and within cirrus. The agreement between relative humidities indicated by DLH
 350 and NWV is excellent, even at the very low mixing ratios encountered during the ATTREX flights.

351 One of the objectives of ATTREX was to investigate how waves affect the TTL cirrus formation
 352 and dehydration processes. RF04 flight was designed to survey horizontal wave structures and
 353 cirrus-wave relationships. An over flight at cruise altitudes of 17.5–18 km along 134–153°E at the
 354 nearly constant latitude of 6°N provided continuous vertical scans of clouds by the onboard down-
 355 looking CPL, as shown in Figure 8. Although ice particles were not detected at the flight altitudes
 356 in this segment due to warmer temperatures than other flights (or upstream regions), the CPL was
 357 able to observe a zonally varying, extensive cirrus layer below flight level. The cloud layer at
 358 $\simeq 12\text{--}16$ km appears to be associated with a 10-day Kelvin wave that was identified by spectral
 359 analysis of radiosonde data at Koror (134°E 7°N) and Chuuk (152°E 7°N). The bottom two panels
 360 of Figure 8 show 7–15 day filtered temperature anomalies at the two radiosonde sites. Koror was
 361 near the coldest phase of the Kelvin wave and Chuuk was near the beginning of the cold phase on
 362 March 6–7, suggesting that the wave had about a zonal wavenumber of 5 ($\simeq 8,000$ km wavelength)
 363 with its peak near Koror and node near Chuuk. The change in the Kelvin wave amplitude likely

induced the change from a thicker persistent cloud layer in the west to a thinner broken cloud layer in the east.

Figure 9 shows an example of tracers measured in the vicinity of Typhoon Faxai on RF03. The CO₂ and CH₄ concentrations between 350 and 370 K potential temperatures measured on this flight (colored data points) were the highest values encountered over the tropical western Pacific. We examined surface measurements at various NOAA stations over the tropical Pacific in order to compare chemical signatures at the surface and the fresh, convectively lofted air. We find that concentrations of both CO₂ and CH₄ from Mauna Loa, HI agree well with the extreme concentrations sampled by the aircraft on this flight, suggesting rapid injection of nearby air from the tropical northern Hemisphere and little contribution from the tropical Southern Hemisphere. Also shown in Figure 9 are CO₂ concentrations sampled at other geographical locations and times during the ATTREX flights from Guam (gray data points). The spread in CO₂ concentrations below 370 K reflects inputs from both the northern and southern hemispheres. Above 370 K, we find reduced variability in CO₂ and a profile shape dictated by the phase of the CO₂ seasonal cycle, namely the gradual build up as the biosphere transitions from photosynthesis to respiration, ascending throughout the TTL over time.

Numerous trace gases were measured by the whole air sampler to better define the composition and variation of organic compounds in the TTL region. ATTREX measurements expanded by over an order of magnitude the available data of organic chemical composition in the TTL region. The gases that were measured included a range of C₂ - C₄ non-methane hydrocarbons, long-lived chlorofluorocarbons and hydrochlorofluorocarbons, various halogenated solvents, selected organic sulfur and nitrogen species, and a full range of halogenated methanes. Compounds of different lifetimes and source emission regions are being used to evaluate mixing, transport, and chemistry in the TTL region. A high priority for the ATTREX mission was to define the input of reactive

bromine to the stratosphere from both short-lived species (such as bromoform, CHBr_3) as well as the longer lived compounds (such as halons and methyl bromide). These measurements (along with ozone) are illustrated in Figure 10. The average concentration of short-lived brominated compounds contribute approximately 18% of the total organic bromine at the tropical tropopause. The data will be used in conjunction with the BrO measurements from the DOAS instrument to examine the total bromine budget and partitioning between organic and inorganic bromine in the TTL and lower stratosphere.

5. Summary and discussion

The 2014 ATTREX deployment to Guam has provided a unique dataset of highly resolved tracer, cloud, water vapor, chemical radical, and radiation measurements in the western Pacific tropical tropopause layer. The wintertime western Pacific TTL is particularly important for controlling stratospheric composition because the coldest tropopause temperatures and strongest vertical ascent rates occur in this region. The six Global Hawk flights from Guam provided surveys of western Pacific TTL composition, measurements in regions recently influenced by deep convection, extensive sampling of TTL cirrus and relative humidity, spectrally-resolved radiative flux measurements, measurements of TTL wave characteristics, and measurements of tracer gradients between the TTL and extratropical lower stratosphere.

The ATTREX measurements are being used for two general types of analyses: (1) phenomenological studies focused on understanding particular physical processes such as TTL transport pathways and rates, ice cloud formation and dehydration, dynamics controlling TTL thermal structure, transport and chemical processes controlling halogen species concentrations; and (2) evaluation and improvement of global-model representations of these TTL processes. The precise, high-resolution tracer measurements in the remote western Pacific provided a wealth of information

about both deep convective and large-scale transport into and through the TTL. The ATTREX measurement suite included tracers with maritime, industrial, biomass-burning, and southern hemisphere sources. The unprecedented accuracy and precision of the water vapor measurements permits quantitative investigations of cloud processes such as ice nucleation, crystal growth, sedimentation, and removal of vapor in excess of saturation. The long Global Hawk flights along with the high occurrence frequency of cirrus in the western Pacific TTL resulted in accumulation of about 34 hours of sampling in clouds. This extensive dataset permits statistical analyses of the cloud properties and humidity in addition to studies of particular cloud events.

The ATTREX data is openly available (<https://espoarchive.nasa.gov/>). However, data users are strongly encouraged to discuss the uncertainties and applicability of the measurements with the instrument leads listed in Table 1. Also, if the measurements are an important component of a scientific study, co-authorship should be offered to the instrument investigators.

Numerous modeling and data analysis activities based on the ATTREX data are currently underway. The measurements are being used both for case-study process studies, such as understanding the processes leading to observed clouds and water vapor concentrations in particular regions (e.g. ??), and for statistical comparison with models. The dataset is proving beneficial for evaluation of global-model representations of transport, chemical processes, and cloud processes. The combined datasets from CAST (lower–middle troposphere), CONTRAST (middle–upper troposphere), and ATTREX (upper troposphere–lower stratosphere) are being used to understand processes controlling short-lived organic and inorganic halogen species. The expectation is that the model improvements based on these analyses will improve the accuracy of climate predictions.

Although the ATTREX measurements have provided an invaluable dataset for studying TTL physical processes, a number of key measurement needs remain. Operational limits prevented the Global Hawk from sampling regions with temperatures colder than about 186 K. Trajectory

calculations indicate that most air parcels transiting through the TTL during Boreal wintertime experience colder temperatures. Measurements of water vapor and cloud properties at the lowest TTL temperatures would be useful for investigating dehydration processes at the point of minimum saturation mixing ratio. The ATTREX payload did not include aerosol measurements, and very little information about TTL aerosol composition and physical properties is available. In particular, direct measurements of ice nuclei concentration and composition in the TTL are needed to definitively determine the relative importance of homogeneous and heterogeneous ice nucleation for production of TTL cirrus ice crystals.

The lack of suitable Global Hawk bases and cost issues prevented the originally planned ATTREX operations in the southeast Asia region during Boreal summertime. Physical processes controlling TTL humidity, clouds, and general composition are likely very different during the summertime “warm phase” of the tropical tropopause seasonal temperature variation. In particular, the summertime TTL and lower stratosphere composition appears to be dominated by convection and radiative heating associated with the Asian monsoon (e.g. ???). Aircraft measurements of TTL properties and physical processes in southeast Asia during Boreal summertime would help address these issues.

Acknowledgments. We would like to thank the Global Hawk project managers, pilots, and crew. Without their hard work overcoming numerous challenges, collection of the excellent data described here would not have been possible. Additional funding from the Deutsche Forschungsgemeinschaft (DFG), grant number PF 384 12/1, in support of the DOAS measurements and data processing is acknowledged.

References

457 **LIST OF TABLES**

458 **Table 1.** Global Hawk Payload 24

459 **Table 2.** ATTREX Guam Global Hawk flights 25

TABLE 1. Global Hawk Payload

Instrument	Investigator	Institution	Measurements
Remote			
Cloud Physics Lidar (CPL)	M. McGill	NASA/GSFC	Aerosol/cloud backscatter
Microwave Temperature Profiler (MTP)	M. Mahoney	JPL/Caltech	Temperature profile
Differential Optical Absorption Spectrometer (DOAS)	J. Stutz, K. Pfeilsticker	UCLA/Univ. Heidelberg	O ₃ , O ₄ , BrO, NO ₂ , OClO, IO H ₂ O, cloud properties
In Situ			
Diode Laser Hygrometer (DLH)	G. Diskin	NASA/LaRC	H ₂ O vapor
NOAA Water (NW)	T. Thornberry, A. Rollins	NOAA/CIRES	H ₂ O (vapor and total)
Hawkeye (2D-S, FCDP, CPI)	P. Lawson	Spec, Inc.	Ice crystal size distributions, habits
NOAA Ozone (NW)	R.-S. Gao	NOAA/CSD	O ₃
Harvard Univ. Picarro Cavity Ringdown Spectrometer (HUPCRS)	S. Wofsy	Harvard Univ.	CO ₂ , CH ₄ , CO
UAS Chromatograph for Tracers (UCATS)	J. Elkins	NOAA/GMD	N ₂ O, SF ₆ , CH ₄ , H ₂ , CO, O ₃ , H ₂ O
Solar and infrared radiometers	P. Pilewskie	Univ. of Colorado	Zenith and nadir radiative fluxes
Meteorological Measurement System (MMS)	P. Bui	NASA/ARC	Temperature, pressure, and winds
Global Hawk Whole Air Sampler (GWAS)	E. Atlas	Univ. of Miami	CFCs, halons, HCFCs, N ₂ O, CH ₄ , HFCs, PFCs, hydrocarbons, etc.

TABLE 2. ATTREX Guam Global Hawk flights

Flight	Date in 2014	Takeoff time, duration	Number of profiles	Science foci
Transit to Guam	16-17 January	04:16 UT, 19.9 hours	1	Transit aircraft to Guam
RF01	12-13 February	17:47 UT, 17.5 hours	30	TTL survey, cirrus sampling
RF02	16-17 February	17:18 UT, 17.7 hours	26	TTL survey, cirrus sampling
RF03	4-5 March	17:28 UT, 12.7 hours	20	Cyclone Faxai sampling, cirrus sampling
RF04	6-7 March	17:00 UT, 17 hours	24	TTL survey, wave measurements
RF05	9-10 March	15:24 UT, 19.7 hours	34	Southern survey, convective outflow
RF06	11-12 March	16:53 UT, 15.3 hours	32	Northern/midlatitude survey
Transit to AFRC	13-14 March	19:53 UT, 19.4 hours	31	Pacific tropical survey, cirrus sampling

LIST OF FIGURES

Fig. 1.	Schematic depiction of TTL physical processes versus longitude and height.	28
Fig. 2.	The Global Hawk unmanned aircraft system. The wing pods, one with the Hawkeye instrument and the other with an aerodynamic/weight dummy for balance, are visible.	29
Fig. 3.	Global Hawk Guam deployment flight paths. Note that for RF02, the aircraft simply profiled over Guam. The paths of 2011 and 2013 ATTREX flights from Armstrong Flight Research Center (AFRC) in southern California are shown (white lines) for context. Average 95 hPa temperatures for the 1 February – 15 March period from ERA-Interim analyses are over-plotted, along with the incidence of infrared brightness temperatures less than 210 K (from geostationary meteorological satellites). In the tropics, 210 K is at 165 hPa, just below the mean altitude of deep convective cloud tops. The colored X's mark the approximate position of the northern hemisphere monsoon anticyclone discussed in the text for the corresponding research flights.	30
Fig. 4.	Latitude, longitude, and height coverage of ATTREX Global Hawk flights. Black curves correspond to ATTREX1 (2011) and ATTREX2 (2013); colored curves show the ATTREX3 flights from Guam. The greyscale background shows the mean temperature versus latitude and height at the Guam longitude (top) and temperature versus longitude and height at the Guam latitude (bottom). Darkest shading indicates mean temperatures approaching 188 K, and lightest shading indicates mean temperatures greater than 205 K.	31
Fig. 5.	RF03 flight path just south of cyclone Faxai.	32
Fig. 6.	Examples of Hawkeye TTL cirrus measurements. 2D-S/FCDP size distributions in two different temperature ranges (left panel) and corresponding CPI ice crystal images (right panel) are shown.	33
Fig. 7.	Top: Frequency distributions of western Pacific TTL relative humidity with respect to ice from DLH (green) and NOAA-WV (blue). Both datasets indicate a peak near 100% corresponding to data inside cirrus as well as common occurrence of supersaturation with respect to ice. Bottom: Ratio of DLH to NWV relative humidity with respect to ice versus the NWV relative humidity.	34
Fig. 8.	Top: CPL clouds from the cruise altitude flight segment along 134–153°E at 6°N in RF04. Arrows indicate the nearby locations of radiosondes (Koror at 134°E 7°N; Chuuk at 152°E 7°N). Bottom left: Radiosonde temperature anomalies filtered with 7–15 day periods for Koror. The asterisk shows the aircraft position and the thin vertical line is the view of the CPL. The dashed line indicates the top of the cirrus layer at about 16 km, which is approximately co-located with the cold-point tropopause. Bottom right: Same as bottom left, but for Chuuk.	35
Fig. 9.	Vertical profiles of CO ₂ as a function of potential temperature for the Tropical Western Pacific (15°N - 12°S) during all ATTREX flights from Guam (grey points). Highlighted in color data from the flight south of the core of Typhoon Faxai on March 4, 2014 (RF03). The color corresponds to CH ₄ concentrations at a given CO ₂ concentration. Also shown are 11-day averages (solid lines) and minima and maxima (dashed lines) of CO ₂ and CH ₄ (color) concentrations at NOAA tropical surface stations in the Northern Hemisphere (Mauna Loa, HI) and the Southern Hemisphere (American Samoa). The 11-day period extends from Feb, 27 to Mar, 9 2014, which corresponds to the lifetime of the typhoon.	36

503 **Fig. 10.** Vertical profiles of selected trace gases measured in the TTL during the ATTREX Guam
 504 flights. The Whole Air Sampler data including a full suite of organic bromine compounds
 505 are shown in the left panel. The very short-lived organic bromine (VSL-Br) species include
 506 CHBr_3 , CH_2Br_2 , CH_2BrCl , CHBr_2Cl , and CHBrCl_2 . Total organic bromine includes the
 507 VSL-Br species plus Halons and CH_3Br . The very short-lived organic bromine compounds
 508 contributed approximately 18% to the total organic bromine at the tropical tropopause. No
 509 systematic influence of latitude was detected in the vertical gradients. Right panel: Ozone
 510 (nmol/mol) data from the UCATS instrument. Individual points are averaged over the sam-
 511 ple integration time of the whole air samples. Ozone profiles tend to be anticorrelated with
 512 organic bromine concentrations in the TTL. 37

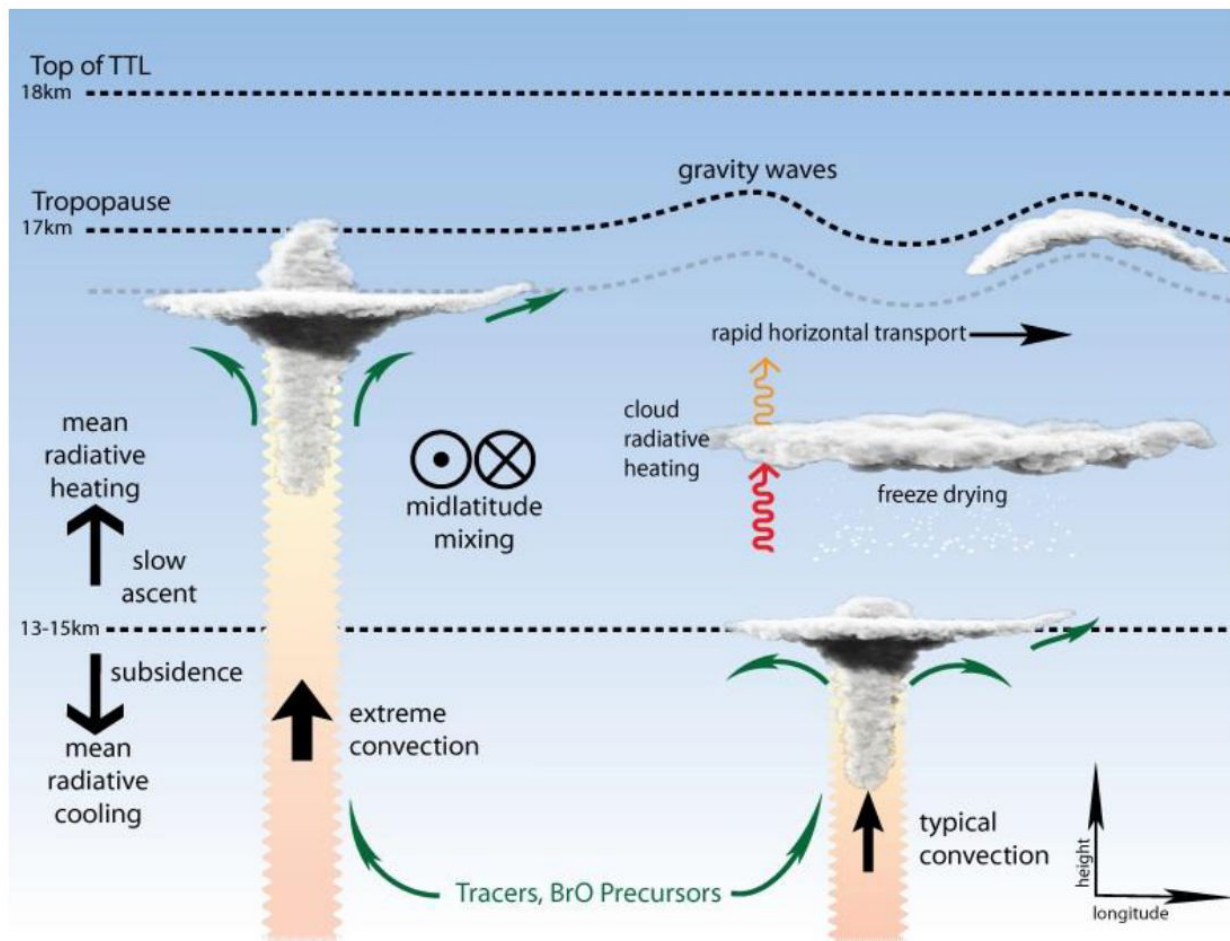


FIG. 1. Schematic depiction of TTL physical processes versus longitude and height.



513 FIG. 2. The Global Hawk unmanned aircraft system. The wing pods, one with the Hawkeye instrument and
514 the other with an aerodynamic/weight dummy for balance, are visible.

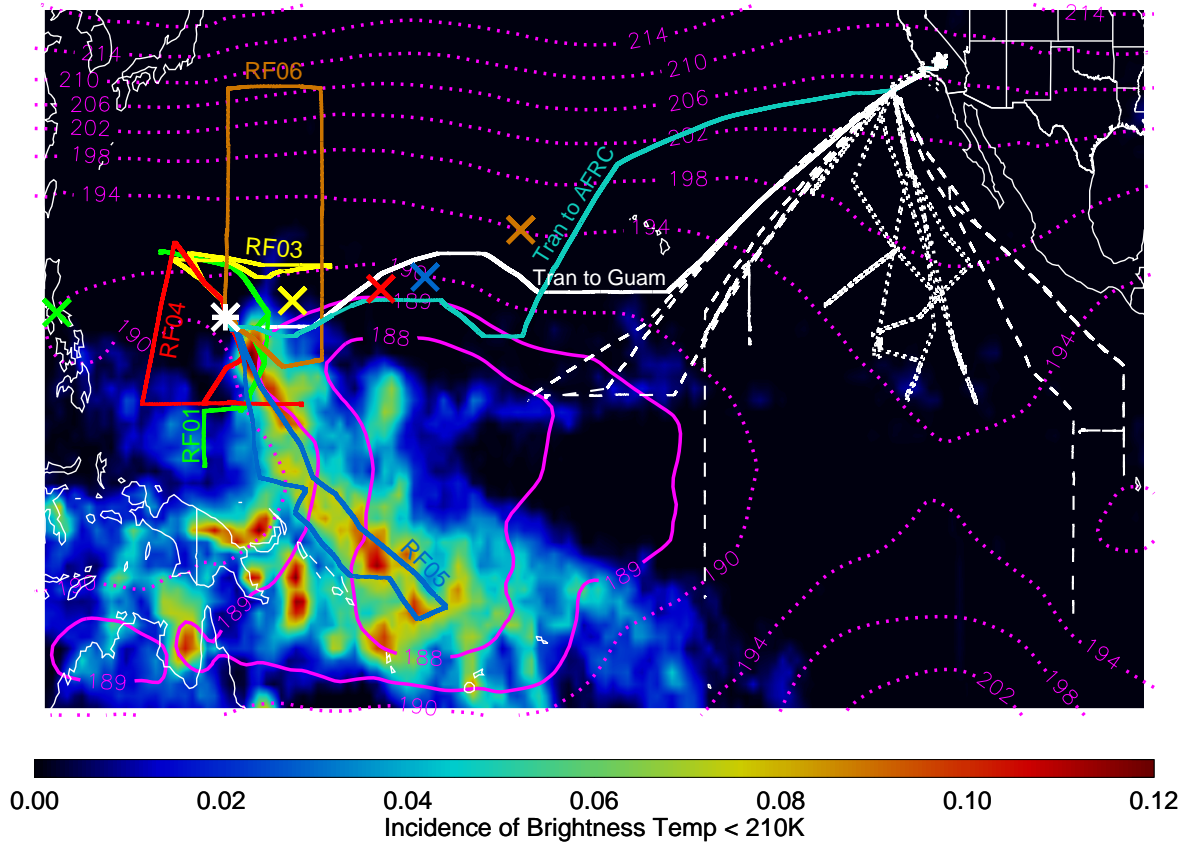


FIG. 3. Global Hawk Guam deployment flight paths. Note that for RF02, the aircraft simply profiled over Guam. The paths of 2011 and 2013 ATTREX flights from Armstrong Flight Research Center (AFRC) in southern California are shown (white lines) for context. Average 95 hPa temperatures for the 1 February – 15 March period from ERA-Interim analyses are over-plotted, along with the incidence of infrared brightness temperatures less than 210 K (from geostationary meteorological satellites). In the tropics, 210 K is at 165 hPa, just below the mean altitude of deep convective cloud tops. The colored X's mark the approximate position of the northern hemisphere monsoon anticyclone discussed in the text for the corresponding research flights.

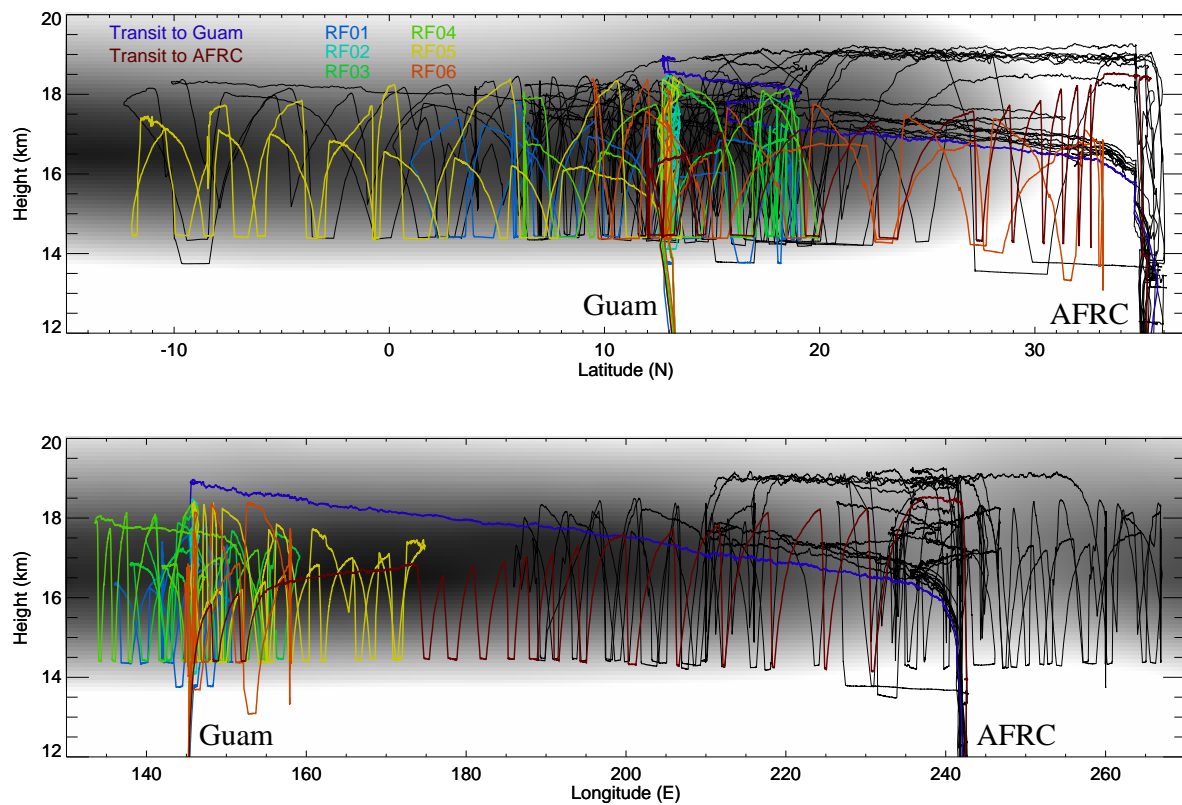


FIG. 4. Latitude, longitude, and height coverage of ATTREX Global Hawk flights. Black curves correspond to ATTREX1 (2011) and ATTREX2 (2013); colored curves show the ATTREX3 flights from Guam. The greyscale background shows the mean temperature versus latitude and height at the Guam longitude (top) and temperature versus longitude and height at the Guam latitude (bottom). Darkest shading indicates mean temperatures approaching 188 K, and lightest shading indicates mean temperatures greater than 205 K.

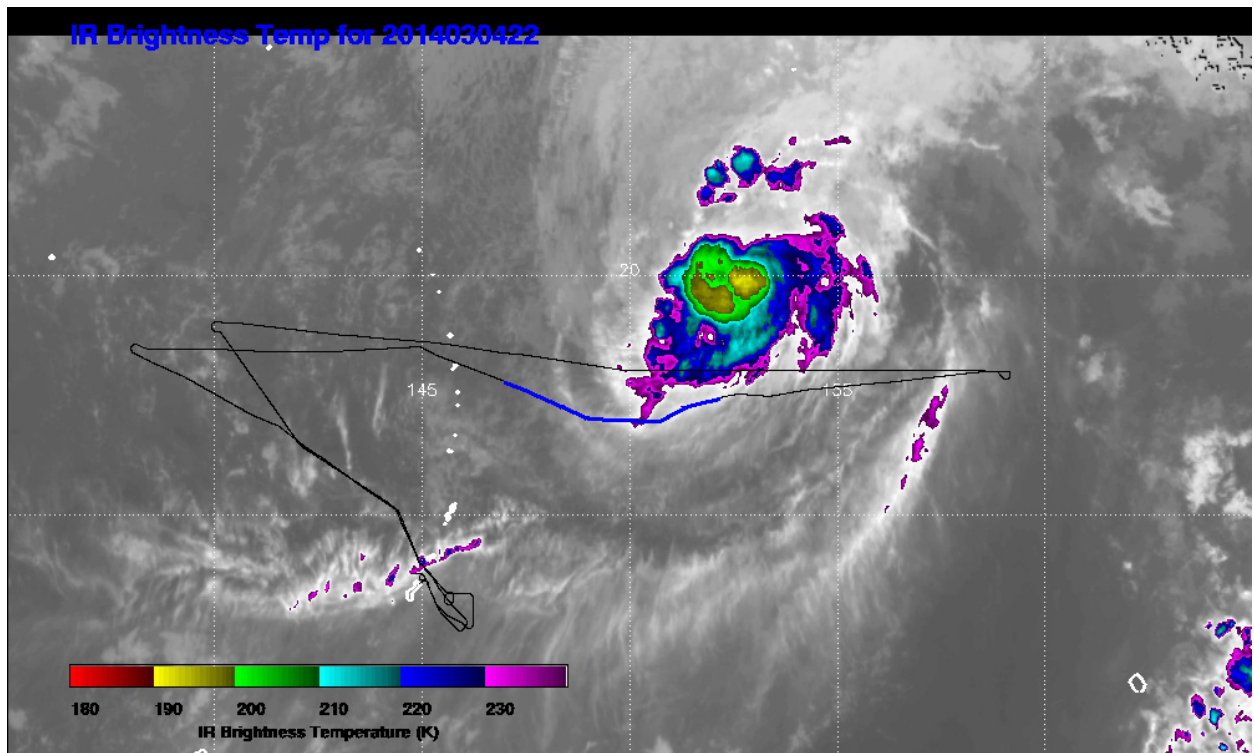


FIG. 5. RF03 flight path just south of cyclone Faxai.

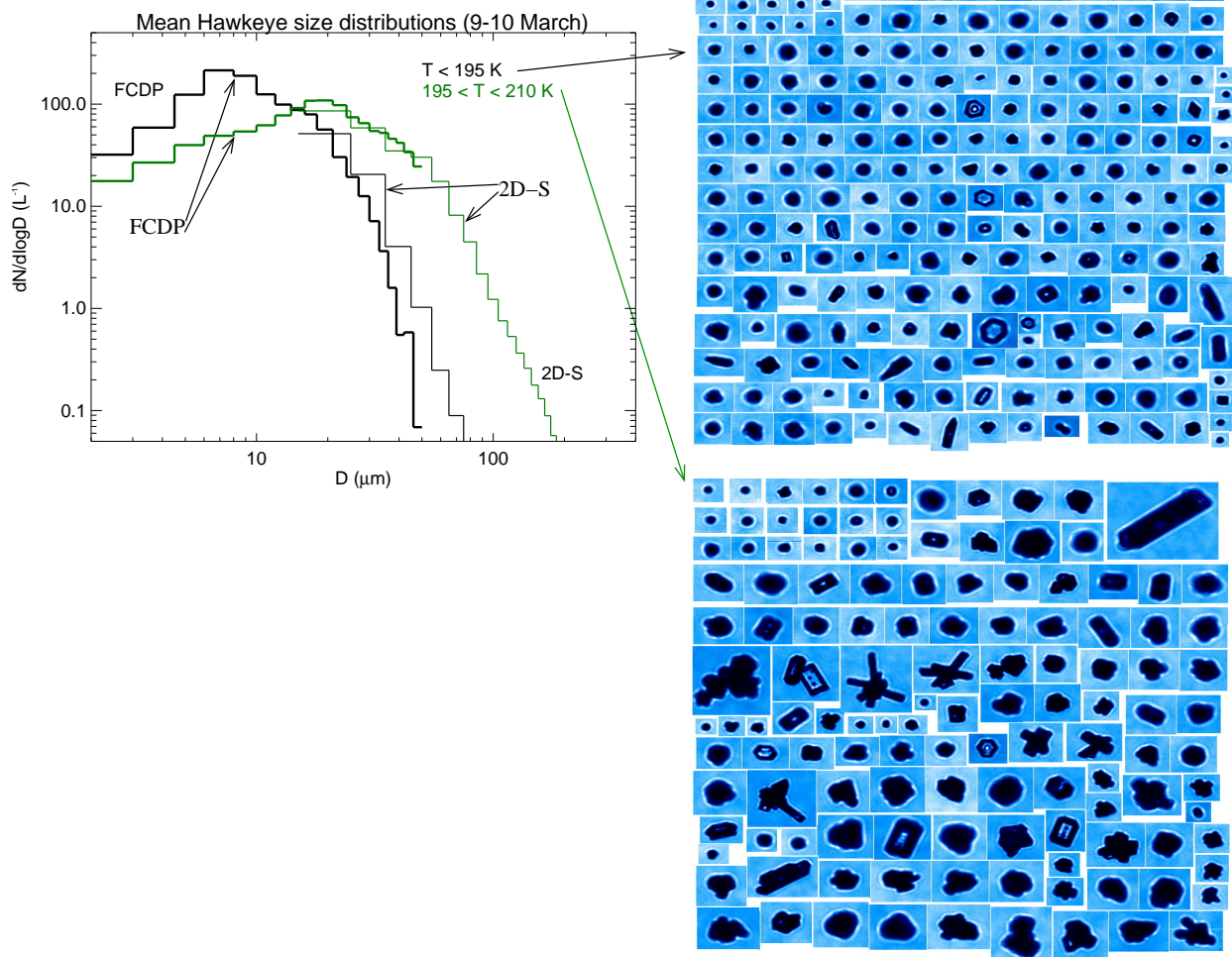


FIG. 6. Examples of Hawkeye TTL cirrus measurements. 2D-S/FCDP size distributions in two different temperature ranges (left panel) and corresponding CPI ice crystal images (right panel) are shown.

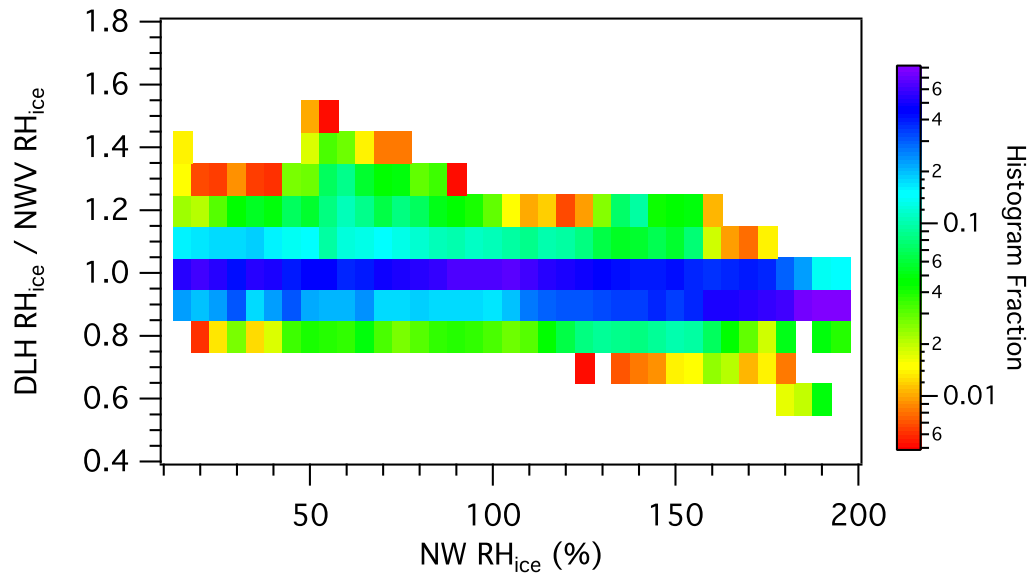
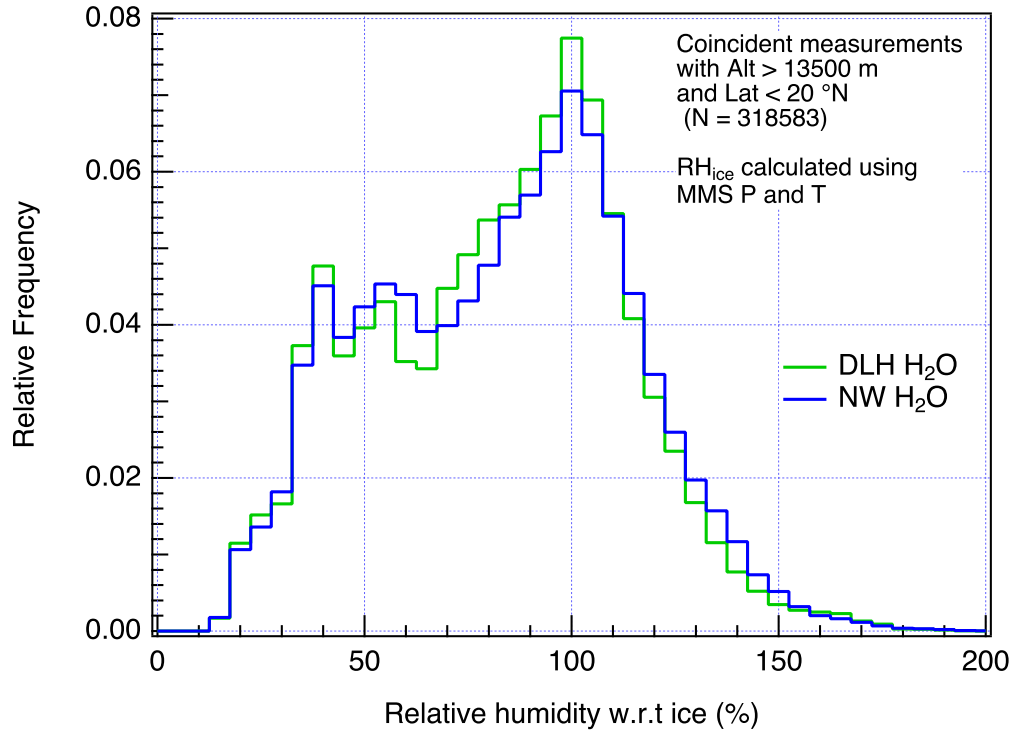


FIG. 7. Top: Frequency distributions of western Pacific TTL relative humidity with respect to ice from DLH (green) and NOAA-WV (blue). Both datasets indicate a peak near 100% corresponding to data inside cirrus as well as common occurrence of supersaturation with respect to ice. Bottom: Ratio of DLH to NWV relative humidity with respect to ice versus the NWV relative humidity.

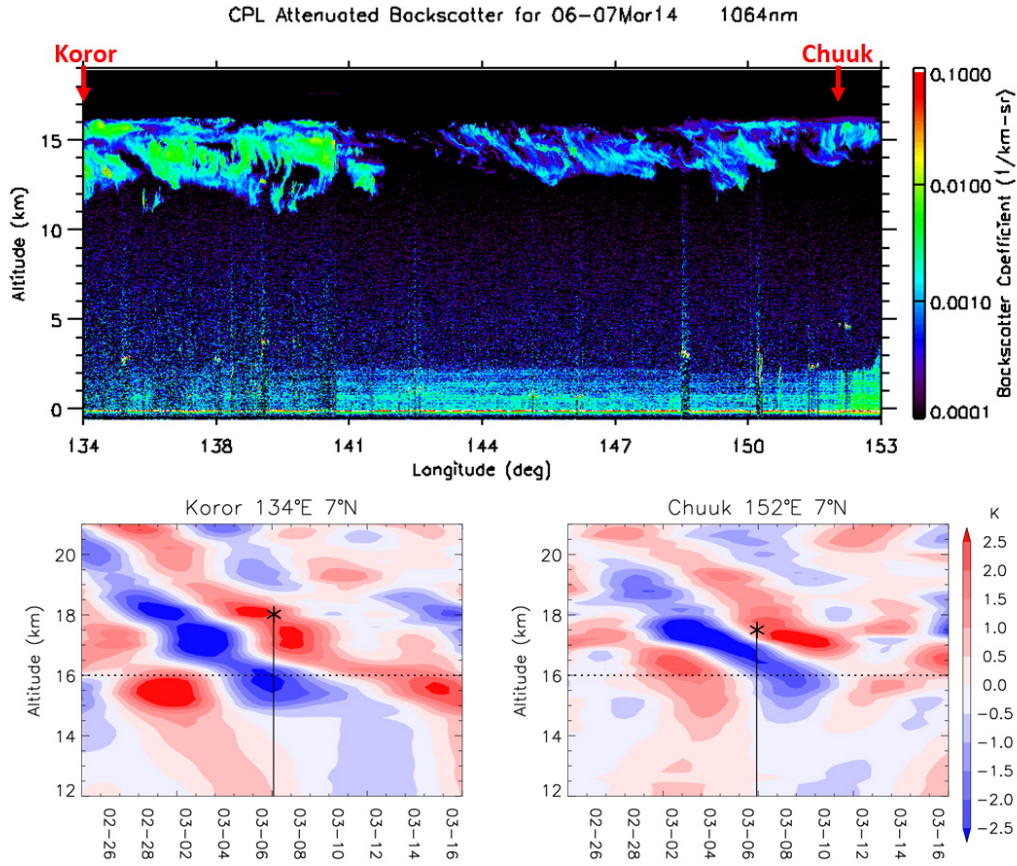
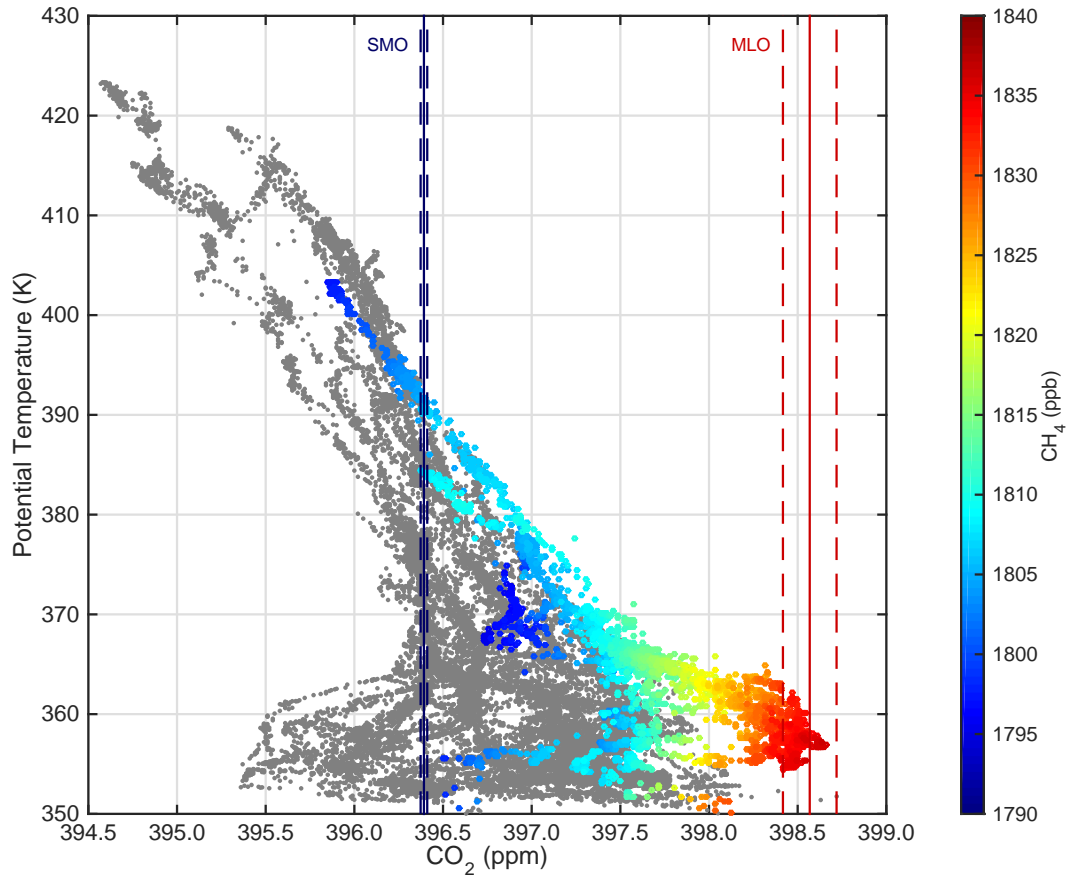


FIG. 8. Top: CPL clouds from the cruise altitude flight segment along 134–153°E at 6°N in RF04. Arrows indicate the nearby locations of radiosondes (Koror at 134°E 7°N; Chuuk at 152°E 7°N). Bottom left: Radiosonde temperature anomalies filtered with 7–15 day periods for Koror. The asterisk shows the aircraft position and the thin vertical line is the view of the CPL. The dashed line indicates the top of the cirrus layer at about 16 km, which is approximately co-located with the cold-point tropopause. Bottom right: Same as bottom left, but for Chuuk.



539 FIG. 9. Vertical profiles of CO₂ as a function of potential temperature for the Tropical Western Pacific (15°N -
 540 12°S) during all ATTREX flights from Guam (grey points). Highlighted in color data from the flight south of the
 541 core of Typhoon Faxai on March 4, 2014 (RF03). The color corresponds to CH₄ concentrations at a given CO₂
 542 concentration. Also shown are 11-day averages (solid lines) and minima and maxima (dashed lines) of CO₂ and
 543 CH₄ (color) concentrations at NOAA tropical surface stations in the Northern Hemisphere (Mauna Loa, HI) and
 544 the Southern Hemisphere (American Samoa). The 11-day period extends from Feb, 27 to Mar, 9 2014, which
 545 corresponds to the lifetime of the typhoon.

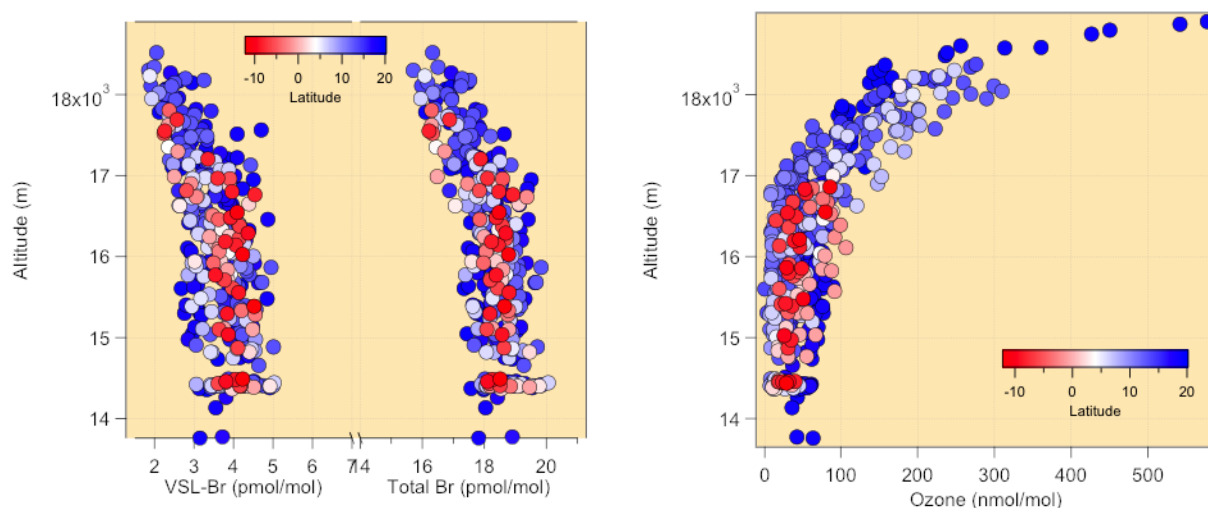


FIG. 10. Vertical profiles of selected trace gases measured in the TTL during the ATTREX Guam flights. The Whole Air Sampler data including a full suite of organic bromine compounds are shown in the left panel. The very short-lived organic bromine (VSL-Br) species include CHBr_3 , CH_2Br_2 , CH_2BrCl , CHBr_2Cl , and CHBrCl_2 . Total organic bromine includes the VSL-Br species plus Halons and CH_3Br . The very short-lived organic bromine compounds contributed approximately 18% to the total organic bromine at the tropical tropopause. No systematic influence of latitude was detected in the vertical gradients. Right panel: Ozone (nmol/mol) data from the UCATS instrument. Individual points are averaged over the sample integration time of the whole air samples. Ozone profiles tend to be anticorrelated with organic bromine concentrations in the TTL.